Solving the eigenvalue problem of the nuclear Yukawa-folded mean-field Hamiltonian[☆]

A. Dobrowolski [a,*], K. Pomorski [a], J. Bartel [b]

[a] *Theoretical Physics Department, Maria Curie-Sklodowska University, Lublin, Poland*
[b] *Institute Pluridisciplinaire H. Curien, Université de Strasbourg, France*

ARTICLE INFO

ABSTRACT

The nuclear Hamiltonian with a Yukawa-folded mean-field potential is diagonalized within the basis of a deformed harmonic-oscillator in Cartesian coordinates. The nuclear shape is characterized by the equivalent sharp surface described either by the well known Funny–Hills or the Trentalange–Koonin–Sierk parametrizations. They are both able to describe a very vast variety of nuclear deformations, including necked-in shapes, left–right asymmetry and non-axiality. The only imposed limitation on the nuclear shape is the z-signature symmetry, which corresponds to a symmetry of the shape with respect to a rotation by an angle π around the z-axis. On output, the computer code produces for a given nucleus with mass number A and charge number Z the energy eigenvalues and eigenfunctions of the mean-field Hamiltonian at chosen deformation.

Program summary

Program title: yukawa

Catalogue identifier: AEYI_v1_0

Program summary URL: http://cpc.cs.qub.ac.uk/summaries/AEYI_v1_0.html

Program obtainable from: CPC Program Library, Queen's University, Belfast, N. Ireland

Licensing provisions: Standard CPC licence, http://cpc.cs.qub.ac.uk/licence/licence.html

No. of lines in distributed program, including test data, etc.: 78599

No. of bytes in distributed program, including test data, etc.: 1551468

Distribution format: tar.gz

Programming language: Fortran 77.

Computer: Any PC machine.

Operating system: Windows or a system based on Linux.

RAM: bytes: 0.5 GB or more

Classification: 17.19.

Nature of problem: The full single-particle nuclear Hamiltonian composed of the Yukawa-folded central, spin–orbit and Coulomb potentials is generated and diagonalized. The only symmetry of the problem is the so called z-signature symmetry which limits the nuclear shapes to those, being invariant with respect to a rotation by an angle π around the z-axis.

Solution method: The mean-field Hamiltonian is expressed in matrix form in the basis of an anisotropic harmonic-oscillator potential written in Cartesian coordinates, where the basis parameters are adjusted to the actual deformed nuclear shape. The eigensolutions of the Hamiltonian are determined by diagonalization of the corresponding matrix.

Running time: For a nucleus of spherical shape, with the inclusion of NMAX = 14 major oscillator shells and including the option of printing out all the eigenfunctions, one program run takes around 7 s on an average dual-core 2 GHz notebook of 1 GB RAM memory. The same type of calculation for a complicated non-axial left–right asymmetric shape requires around 11 s.

1. Introduction

One of the basic problems of theoretical nuclear physics consists in getting a realistic description of the structure of the nuclear N-particle system as a function of its deformation. For several decades the *macroscopic–microscopic model* has played a predominant role in this context. Nowadays, microscopic approaches of the selfconsistent mean-field type (Hartree–Fock, Hartree–Fock–Bogoliubov, etc.) based on some effective nucleon–nucleon interactions have become quite performant and have the advantage that the self-consistent mean-field is determined by the solutions of the eigenvalue problem of the Hamiltonian. In spite of the undeniable success of such selfconsistent mean-field methods, the macroscopic–microscopic approach is still useful to obtain reliable estimates of nuclear properties, in particular in the context of large-scale nuclear structure calculations, where the selfconsistent methods are often much more time consuming. As an example one can give by nuclear deformation-energy landscape of nuclei which require to perform many selfconsistent mean-field calculations under the constraint of some deformation measure, like the mass quadrupole and higher multipolarity moments. An illustrative example is e.g. given by the deformation-energy landscape of a nucleus obtained under the constraint of the mass quadrupole and/or some higher multipole moments. To obtain such a deformation-energy landscape in a selfconsistent method would require a very large number of constrained mean-field calculations. To perform such a calculation for a single nucleus but for more than two such constraints is already very demanding, to make it for a whole nuclear region is a task addressed for powerful multiprocessor computer clusters. To perform such calculations within a selfconsistent mean-field approach is, even today, hardly possible for the *average* physicist. Such a calculation is, however, often performed in the context of the macroscopic–microscopic model as demonstrated in Ref. [1].

The basis of such a macroscopic–microscopic method is a liquid-drop, droplet (LD) or any other macroscopic model of atomic nuclei that is able to yield, together with the microscopic energy corrections, to be discussed in detail below, not only realistic nuclear masses, but also realistic nuclear energies as functions of the shape of nuclear surface, in particular, fission barrier heights [2]. These purely quantal-type (shell and pairing energy) corrections are calculated for a given nucleus on the basis of single-particle energy spectra which may change considerably as function of the nuclear shape. It is also obvious that the knowledge of the nuclear mean-field Hamiltonian and its eigensolutions is crucial as basis for an appropriate treatment of dynamic nuclear processes like nuclear fission, fusion, rotations, collective excitations as giant resonances and so on.

2. Descriptions of the nuclear surface

One of the basic problems in nuclear mean-field theory based on the macroscopic–microscopic Strutinsky model [3] is the adequate description of nuclear shapes. Within the macroscopic–microscopic approach the nuclear shape is usually understood as the **presupposed** shape of the surface, where for example, the density of nucleons reaches half of its saturation density. One should remember that density fluctuations due to intrinsic nuclear shell structure are neglected. In addition, the nuclear surface, defined in this way, differs, in general, from the surface defined by the mean-field potential. This point is developed in more details in the following.

In the mean-field model study of heavy-ion reactions, of nuclear fusion and fission phenomena, nuclear rotations and collective vibrations, the nuclear potential energy surface (PES) plays a key role. It is therefore clear that the parametrization of the nuclear shape used to generate the PES needs to be both simple and flexible, i.e. involving only a few relevant collective deformation parameters, corresponding to degrees of freedom that have identified from long-standing experience in this kind of studies. Those parameters should allow for a reliable description of the large variety of nuclear forms occurring in the description of above quoted phenomena. For example, in the case of the nuclear fission process, some crucial geometric degrees of freedom are the elongation of the nucleus, the width of the neck and, for certain regions of nuclei or nuclear deformations, the mass asymmetry and nonaxiality.

In the following nuclear shapes are described in terms of the famous "*Funny–Hills*" (FH) [4] as well as the so-called *Trentalange–Koonin–Sierk*" (TKS) nuclear shape parametrizations [5]. In the latter, the nuclear surface is developed in the series of Legendre polynomials, as explained in detail below.

2.1. Funny–Hills shapes

A very efficient parametrization of the nuclear surface, in particular in the description of the nuclear fission process, was proposed in Ref. [4]. It describes the axially-symmetric nuclear surface in cylindrical coordinates as a function of three independent parameters $\{A, B, \alpha\}$ and the two parameters $\{z_0, z_{sh}\}$ depending, in general on the above three, as:

$$\rho_s^2(u) = \begin{cases} R_0^2 c^2 \left(1 - u^2\right) \left[A + \alpha u + B u^2\right], & B \geq 0 \\ R_0^2 c^2 \left(1 - u^2\right) \left[A + \alpha u\right] \exp(B c^3 u^2), & B < 0. \end{cases} \quad (1)$$

Above, $\rho_s(z)$ is the distance of the nuclear surface from the symmetry axis (chosen as the z-axis) and R_0 is the radius of the spherical nucleus having the same volume as the deformed one. According to Ref. [6] we shall assume in the following that

$$R_0 = 1.16 \left(1 + \bar{\epsilon}\right),$$

$$\bar{\epsilon} = -0.147/A^{1/3} + 0.33 \left(\frac{N - Z}{A}\right)^2 + 0.00248 \, Z^2/A^{4/3}. \quad (2)$$

The dimensionless coordinate u is defined as

$$u = \frac{z - z_{sh}}{z_0}, \quad (3)$$

where $z_0 = c R_0$ is a measure of the elongation of the nuclear shape, such that $2 z_0$ is the distance between the left and right end points

z_{min} and z_{max}. The parameter z_{sh} ensures that the nuclear centre of mass is always localized at $z = 0$, i.e.

$$z_{cm} = \frac{2\pi \int_{z_{min}}^{z_{max}} \rho_s^2(z) z \, dz}{2\pi \int_{z_{min}}^{z_{max}} \rho_s^2(z) \, dz}$$

$$= \frac{R_0 c \int_{-1}^{1} (1 - u^2)(A + \alpha u + B u^2) u \, du}{\int_{-1}^{1} (1 - u^2)(A + \alpha u + B u^2) \, du} = 0,$$ (4)

what yields

$$z_{sh}(c, \alpha) = -\frac{1}{5} \alpha c^3 z_0.$$ (5)

In Eq. (4), the positions of end points of the (in the most general case) left–right asymmetric shape are at $z_{min} = -z_0 + z_{sh}$ and $z_{max} = z_0 + z_{sh}$, which in the case of left–right symmetry obviously become $z_{min} = -z_0$ and $z_{max} = z_0$.

The volume conservation condition

$$V = \frac{4\pi}{3} R_0^3 = \int_0^{2\pi} d\varphi \int_{z_{min}}^{z_{max}} dz \int_0^{\rho_s(z)} \rho \, d\rho$$

$$= z_0 c^2 R_0^2 \pi \int_{-1}^{1} (1 - u^2)(A + \alpha u + B u^2) \, du$$ (6)

allows to determine the elongation parameter c as function of A and B as

$$c(A, B) = \left(A + \frac{1}{5} B\right)^{-1/3}.$$ (7)

The parameter c measures simply the length of the nucleus in units of the radius R_0.

Observe that for $\alpha = 0$ left–right symmetric shapes are obtained and the shift parameter z_{sh} vanishes. The meaning of the α deformation parameter can therefore be associated with the asymmetry of the shape with respect to the XOY plane, thus producing octupole type shapes. Notice (see Eq. (7)) that the elongation c is independent of the left–right asymmetry parameter α.

Usually, an axially-symmetric shape in the Funny–Hills parametrization is defined by means of $\{c, h, \alpha\}$ parameters, where c and α are defined above, while the parameter h, that has not been introduced yet, can be expressed through the neck B and elongation c parameters by the relation

$$h(B, c) = \frac{1}{2} B - \frac{1}{4}(c - 1).$$ (8)

It has been chosen such that $h = 0$ corresponds in the $\{c, B\}$ plane approximately to the average liquid-drop path to fission. The latter corresponds to the curve in the liquid-drop deformation-energy surface along which the liquid-drop energy is minimal for different elongation c and which goes from the spherical minimum ($c = 1$, $B = 0$) through a saddle point towards the scission configuration. The use of $\{c, h, \alpha\}$ deformations given as the combinations of $\{A, B, \alpha\}$ turns out to be convenient, notably for the description of the nuclear fission process due to their intuitive meaning as the elongation in R_0 units along z-axis, the width of the neck (a parameter absolutely necessary to obtain the two-fragment scission configuration) and the left–right asymmetry parameters, respectively. The fact that, for negative B values, a slightly different form (containing the exponential) of the shape function $\rho_s^2(u)$ has been used in (1) is due to the fact that the purely polynomial form turns out to be insufficient for the description of prolate, compact and convex (diamond-like) shapes which occur near the ground state of some (e.g. actinide) nuclei. For the description of the nuclear fission process of e.g. transuranic nuclei, and for substantially elongated ($c \geq 1.3$) non-compact, necked-in shapes
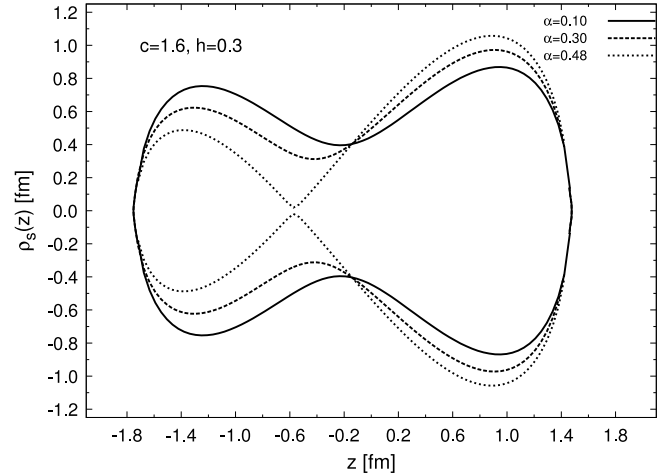
Fig. 1. Variety of nuclear shapes that can be reproduced by the shape parametrization of Eq. (1).

far beyond the ground state, only the polynomial form in (1) will, however, come into play. The two definitions in (1) are, of course, joined smoothly [4].

The large variety of nuclear shapes that can be obtained with the nuclear shape parametrization of Eq. (1) is visualized in Fig. 1 (see also Fig. 5 of Ref. [7]).

Even if the shapes shown in these figures seem to cover a large variety of nuclear deformations, one may question the ability of the shape parametrization (1) to yield deformation energies that are close to the experiment. Through the work of F. Ivanyuk (see [8] and references therein) we know, however, that these Funny–Hills shapes are, indeed, very close to the so-called Strutinsky "*optimal shapes*" that are obtained through a variational principle [9]. What nuclear fission barriers are concerned, we also know that the Funny–Hills shapes give an excellent description of barrier heights in the actinide region as has been demonstrated in Ref. [10] through liquid-drop fission barrier of ^{232}Th obtained with the Funny–Hills shapes, Eq. (1) and, in comparison, with an expansion of the nuclear shape in spherical harmonics, which constitutes an expansion in a basis that can be truncated at any order. It thus turns out that one needs in this expansion to include terms $Y_{\ell m}$ beyond $\ell = 12$ to obtain a description of the barrier that yields a barrier height lower than the one obtained with the Funny–Hills shapes.
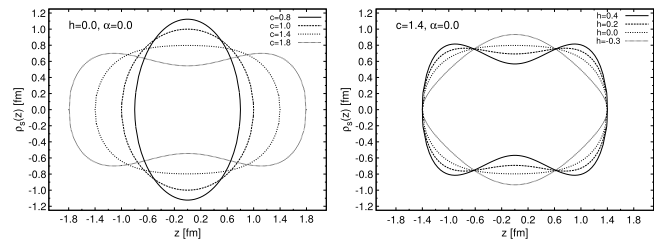
2.2. Trentalange–Koonin–Sierk shapes parametrization

The Funny–Hills shapes are described through the surface shape function $\rho_s^2(z)$ that is given, except for diamond-like shapes, by a fourth order polynomial in the dimensionless coordinate $u = (z - z_{sh})/z_0$ defined in Eq. (3). This can be understood as an expansion of the function $\rho_s^2(u)$ in the basis of powers of u which is truncated at fourth order. One could also imagine other basis functions for such an expansion, like e.g. Legendre polynomials. Following this idea presented by Trentalange, Koonin and Sierk in Ref. [5] we write the

shape function $\rho_s^2(z)$ in the form

$$\rho_s^2(u) = R_0^2 \sum_{n=0}^{N} \alpha_n P_n(u),$$ (9)

where the dimensionless coordinate u is given by Eq. (3) and $P_n(u)$ is the Legendre polynomial of the nth order. The elongation parameter z_0 and the centre-of-mass shift parameter z_{sh}, are defined in the same way, as for the Funny–Hills shapes. The advantage of this Trentalange–Koonin–Sierk (TKS) parametrization consists in the fact that one is not limited to a given form as in (1) and that this expansion can be truncated at any order N. Since the end points of the shape are located at $z_{min} = z_{sh} - z_0$ and $z_{max} = z_{sh} + z_0$, one obtains, taking advantage of the fact that $P_n(1) = 1$ and $P_n(-1) = (-1)^n$, the following relations:

$$\alpha_0 = - \sum_{n=2,4,\ldots} \alpha_n \quad \text{and} \quad \alpha_1 = - \sum_{n=3,5,\ldots} \alpha_n,$$ (10)

which fixes e.g. the two lowest-order parameters. The fact that upon deformation the shape should keep its volume fixed

$$V = \frac{4\pi}{3} R_0^3 = \int_0^{2\pi} d\varphi \int_{z_{min}}^{z_{max}} dz \int_0^{\rho_s(z)} \rho \, d\rho$$

$$= \pi R_0^2 \int_{z_{min}}^{z_{max}} \sum_{n=0}^{\infty} \alpha_n P_n \left(\frac{z - z_{sh}}{z_0} \right) dz$$

$$= \pi R_0^2 z_0 \int_{-1}^{1} \sum_{n=0}^{\infty} \alpha_n P_n(u) \, du = 2\pi R_0^2 z_0 \, \alpha_0$$ (11)

determines the elongation parameters z_0 or c through α_0

$$z_0 = \frac{2}{3} \frac{R_0}{\alpha_0} \quad \Longleftrightarrow \quad c = \frac{z_0}{R_0} = \frac{2}{3\alpha_0},$$ (12)

where we have used the orthogonality relation of Legendre polynomials

$$\int_{-1}^{1} P_\ell(x) P_{\ell'}(x) \, dx = \frac{2}{2\ell + 1} \delta_{\ell\ell'}.$$ (13)

In the presence of deformations including odd multipolarities one has to introduce an additional condition which fixes the position of the mass centre of the deformed shape at the origin of the coordinate system:

$$z_{cm} = \frac{\int_V z \, d^3 r}{\int_V d^3 r} = \frac{\pi \int_{z_{min}}^{z_{max}} \rho_s^2(z) z \, dz}{\pi \int_{z_{min}}^{z_{max}} \rho_s^2(z) \, dz} = 0,$$ (14)

what together with (9) leads to

$$\pi R_0^2 \int_{z_{min}}^{z_{max}} z \sum_{n=0}^{\infty} \alpha_n P_n \left(\frac{z - z_{sh}}{z_0} \right) dz$$

$$= \pi R_0^2 z_0 \int_{-1}^{1} (z_0 u + z_{sh}) \sum_{n=0}^{\infty} \alpha_n P_n(u) \, du = 0.$$

This allows to evaluate the shift z_{sh} as

$$z_{sh} = -\frac{1}{3} \frac{\alpha_1}{\alpha_0} z_0 = -\frac{2}{9} \frac{\alpha_1}{\alpha_0^2} R_0.$$ (15)

As an example we show an explicit expression for nuclear shapes including up to hexadecapole deformations. To that aim, let us specifically consider $\{\alpha_2, \alpha_3, \alpha_4\}$ deformations. The nuclear shape (9) is then described by a fourth-order polynomial in u:

$$\rho_s^2(u) = R_0^2 \left[\alpha_0 - \frac{1}{2}\alpha_2 + \frac{3}{8}\alpha_4 + \left(\alpha_1 - \frac{3}{2}\alpha_3 \right) u \right.$$

$$\left. + \left(\frac{3}{2}\alpha_2 - \frac{15}{4}\alpha_4 \right) u^2 + \frac{5}{2}\alpha_3 u^3 + \frac{35}{8}\alpha_4 u^4 \right].$$ (16)

Some example of shapes described by Eq. (16) are presented in Fig. 2. Using Eqs. (10) one can rewrite the last equation in a form similar to Eq. (1):

$$\rho_s^2(u) = R_0^2(1 - u^2) \left(-\frac{3}{2}\alpha_2 - \frac{5}{8}\alpha_4 - \frac{5}{2}\alpha_3 u - \frac{35}{8}\alpha_4 u^2 \right)$$ (17)

to find, in this very special case a relation between the set of deformation parameters of the Funny–Hills, Eq. (1) and the TKS parametrization, Eq. (9):

$$A = \left(-\frac{3}{2}\alpha_2 - \frac{5}{8}\alpha_4 \right) c^{-2}$$

$$\alpha = -\frac{5}{2}\alpha_3 c^{-2}$$ (18)

$$B = -\frac{35}{8}\alpha_4 c^{-2}.$$

The 4th order polynomial (17) has the following roots:

$$u_{1,2} = \pm 1 \quad \text{and} \quad u_{3,4} = \frac{-4\alpha_3 \mp 4\sqrt{\alpha_3^3 - \frac{21}{5}\alpha_2\alpha_4 - \frac{7}{4}\alpha_4^2}}{7\alpha_4}.$$ (19)

The first two solutions correspond to the tips of the nucleus at $u = \pm 1$, while the next two correspond, in the case $u_3 = u_4$, to the scission configuration which leads then to the following equation for the scission line:

$$\alpha_3^3 - \frac{21}{5}\alpha_2\alpha_4 - \frac{7}{4}\alpha_4^2 = 0.$$ (20)

When $u_3 \neq u_4$ one may obtain either two separated fragments with a region of negative (unphysical) ρ_s^2 values between them, or, in the case of complex roots u_3, u_4 some unphysical shapes when $\rho(0) > 0$ and $u_{3,4}^2 < 1$. This last condition yields an equation for the line which separates "allowed" (physical) and "forbidden" (unphysical) shapes.

As already mentioned above, the average liquid drop path to fission corresponds roughly to $h = 0$, so that one can estimate the parameters $(\alpha_2^{fiss.}, \alpha_4^{fiss.})$ along the scission line as:

$$\alpha_2^{fiss.} = -\frac{2}{3c} + \frac{4}{35}(c - 1)c^2$$ (21)

$$\alpha_4^{fiss.} = -\frac{4}{35}(c - 1)c^2.$$

2.3. Nonaxial case

Neither the Funny Hills, Eq. (1), nor the Trentalange–Koonin–Sierk parametrization, Eq. (9), presented above is able, as such, to describe three-axial shapes which appears, e.g. in some actinide nuclei on their path to fission, in the vicinity of the first barrier. In order to be able to consider also non-axial shapes, let us assume, to simplify the description, that the cross section of the deformed liquid drop perpendicular to the symmetry z-axis is of the form of an ellipse with half axes a and b

$$\frac{x_s^2}{a^2} + \frac{y_s^2}{b^2} = 1.$$ (22)

In polar coordinates the above equation reads

$$\rho_s^2 = \frac{a^2 b^2}{b^2 \cos^2(\varphi) + a^2 \sin^2(\varphi)}.$$ (23)

One can introduce now the non-axiality deformation parameter η defined as

$$\eta = \frac{b^2 - a^2}{a^2 + b^2},$$ (24)
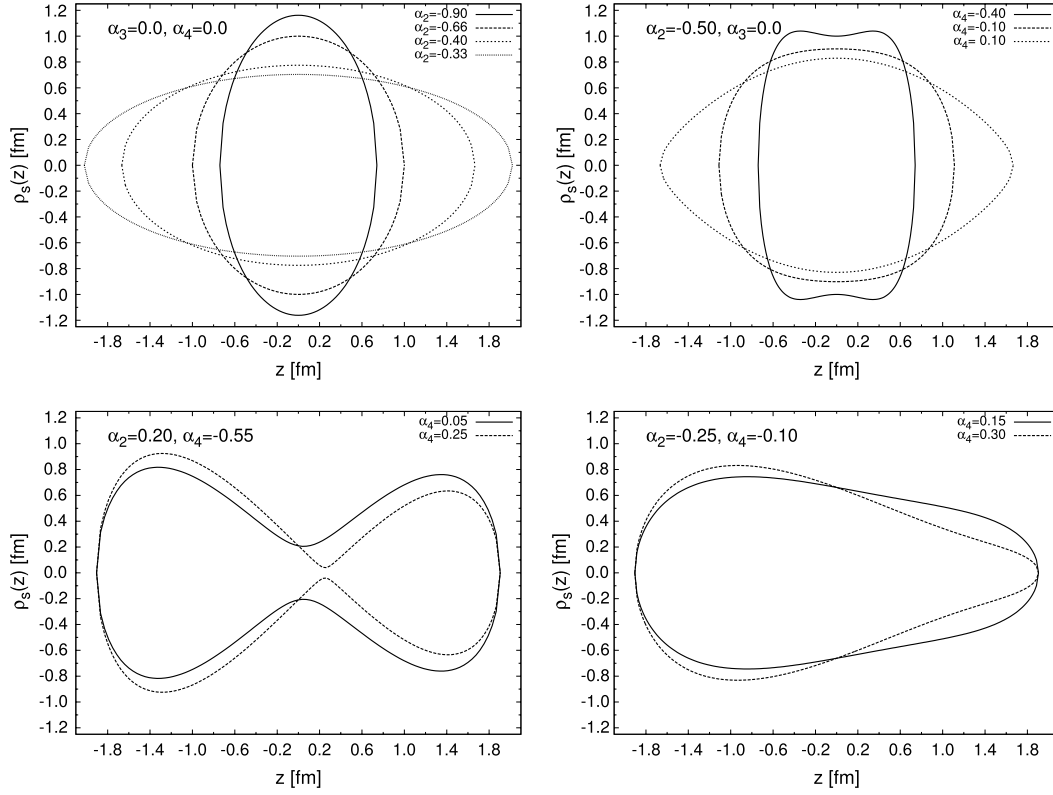
Fig. 2. Variety of nuclear shapes that can be reproduced by the shape parametrization of Eq. (16).

which defines the importance of the nonaxiality of the drop. In order to keep the same volume, Eq. (6), as for the axial case, one assumes that the value of the surface of the ellipse (22) at given z value is independent of the parameter η, i.e.

$$\pi \rho_s^2 = \pi ab, \tag{25}$$

where ρ_s^2 is given e.g. by Eq. (1) or (9). The half axis of the cross section of the shape at given z are therefore of the form

$$a = \rho_s(z) \left(\frac{1-\eta}{1+\eta} \right)^{1/4},$$

$$b = \rho_s(z) \left(\frac{1+\eta}{1-\eta} \right)^{1/4}. \tag{26}$$

Finally, after exploiting the constant-volume condition (6), the square distance of an arbitrary surface point (z, φ) to the z-axis is given by

$$\widetilde{\rho}_s^2(z, \varphi) = \rho_s^2(z) \, \frac{\sqrt{1-\eta^2}}{1 + \eta \cos(2\varphi)}. \tag{27}$$

The non-axiality parameter η defined in (24) could, in general, depend on z but, to simplify the description, we assume in the following that it is z-independent.

2.4. Ellipsoidal case for Funny–Hills shapes

For a vanishing neck parameter, $B = 0$, Eq. (27) describes a pure spheroid with the following main half axes:

$$\mathcal{A} = R_0/\sqrt{c} \left(\frac{1-\eta}{1+\eta} \right)^{1/4},$$

$$\mathcal{B} = R_0/\sqrt{c} \left(\frac{1+\eta}{1-\eta} \right)^{1/4},$$

$$\mathcal{C} = R_0 \, c. \tag{28}$$
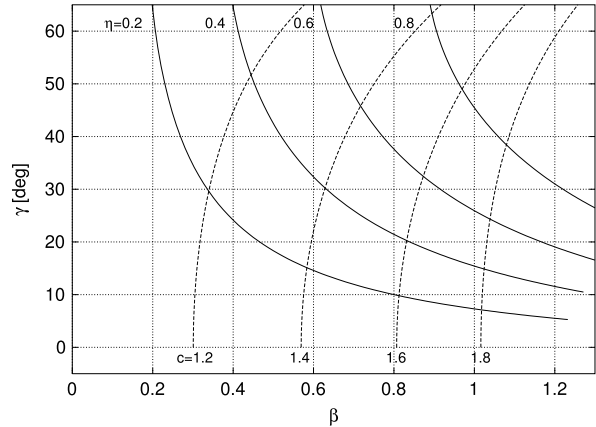
Fig. 3. Transformation from the (β, γ) to (c, η) coordinates for FH shapes in the pure spheroidal case.

In the traditional quadrupole Bohr (β, γ) parametrization these axes are expressed as [11]

$$\mathcal{A} = R(\beta, \gamma) \left[1 - k \cos(\gamma - \pi/3) \right],$$

$$\mathcal{B} = R(\beta, \gamma) \left[1 - k \cos(\gamma + \pi/3) \right],$$

$$\mathcal{C} = R(\beta, \gamma) \left[1 + k \cos(\gamma) \right], \tag{29}$$

where $k = \sqrt{\frac{5}{4\pi}} \, \beta$ and

$$R(\beta, \gamma) = R_0 \left([1 - k \cos(\gamma - \pi/3)] \, [1 - k \cos(\gamma + \pi/3)] \right.$$
$$\left. \times \, [1 + k \cos(\gamma)] \right)^{-1/3}. \tag{30}$$

The transformations between the coordinates $\{c, \eta\}$ and $\{\beta, \gamma\}$ are shown (both ways) in Fig. 3.

3. Folded Yukawa density and mean-field nuclear potential

A diffuse proton and neutron density distribution can be generated, from any sharp edged shape, in the most general way with the help of a folding procedure presented in details in Ref. [12] as

$$\rho(\vec{r}) = \rho_0 \int_V d^3 r' \, g(|\vec{r} - \vec{r}\,'|), \tag{31}$$

where ρ_0 is the uniform density distribution and integration is over a sharp-edge surface enclosing a volume V such that

$$\int_V \rho_0 \, d^3 r = \rho_0 V = \mathcal{N}, \quad \mathcal{N} = N \text{ or } Z. \tag{32}$$

The volume V over which the above integrations extend can be defined by any of the shape functions (1), (9) or (27), or any other shape defined in a similar way. In this way a diffuse-surface density distribution of arbitrary shape can be generated. The folding function in Eq. (31) that produces such a diffuse-surface density needs, obviously, to be normalized

$$\int_{-\infty}^{\infty} g(\vec{r}) \, d^3 r = 1, \tag{33}$$

where integration is over the whole space. The folding function $g(|\vec{r}_1 - \vec{r}_2|)$ can e.g. be chosen to be of the form of the Yukawa function with a width parameter a that will be of the order of the pion Compton wavelength

$$g(|\vec{r}_1 - \vec{r}_2|) = \frac{1}{4\pi a^3} \frac{e^{-|\vec{r}_1 - \vec{r}_2|/a}}{|\vec{r}_1 - \vec{r}_2|/a}. \tag{34}$$

The length of the vector $|\vec{r}_1 - \vec{r}_2|$ can be expressed in cylindrical (ρ, φ, z) coordinates as

$$|\vec{r}_1 - \vec{r}_2| = \sqrt{\rho_1^2 + \rho_2^2 - 2\rho_1\rho_2 \cos(\varphi_1 - \varphi_2) + (z_1 - z_2)^2}. \tag{35}$$

Let us insist here on the fact that the function $g(|\vec{r}_1 - \vec{r}_2|)$ should not be misunderstood as to represent the interaction potential between two nucleons, but rather that a short-range interaction between the constituents of an N-particle system will generate a density distribution with a diffuse surface, where this surface diffuseness should be of the order of the interaction length of the nucleon–nucleon force, i.e. of the order of 1 fm.

3.1. Coulomb potential

Having defined a diffuse-surface density and charge distribution through Eq. (31), the Coulomb interaction potential can be calculated as (see, e.g. Ref. [12])

$$\begin{aligned} V_c(\vec{r}_1) &= e \int_V d^3 r_2 \, \frac{\rho(\vec{r}_2)}{|\vec{r}_1 - \vec{r}_2|} \\ &= e \, \rho_0 \int_V d^3 r_3 \int_V d^3 r_2 \, \frac{1}{|\vec{r}_1 - \vec{r}_2|} \, g(|\vec{r}_2 - \vec{r}_3|). \end{aligned} \tag{36}$$

Using the folding theorem (see, e.g. Ref. [13])

$$\begin{aligned} &\int_{-\infty}^{\infty} d^3 r_2 \, f(\vec{r}_1 - \vec{r}_2) \, g(\vec{r}_2 - \vec{r}_3) \\ &= \int_{-\infty}^{\infty} d^3 k \, \hat{f}(\vec{k}) \, \hat{g}(\vec{k}) \, e^{i\vec{k}(\vec{r}_1 - \vec{r}_3)}, \end{aligned} \tag{37}$$

where $\hat{f}(\vec{k})$ and $\hat{g}(\vec{k})$ are the Fourier transforms of $f(\vec{r}_{12})$ and $g(\vec{r}_{23})$, one obtains for the Coulomb potential of Eq. (36)

$$V_c(\vec{r}_1) = \frac{4\pi e \rho_0}{(2\pi)^{3/2}} \int_V d^3 r_3 \int_{-\infty}^{\infty} d^3 k \, \frac{1}{k^2} \, \hat{g}(\vec{k}) \, e^{i\vec{k}(\vec{r}_1 - \vec{r}_3)}, \tag{38}$$

where it turns out that the Fourier transform $\hat{g}(k)$ of $g(|\vec{r}_{23}|)$ depends, because of the specific form of $g(|\vec{r}_{23}|)$, only on the magnitude of $\vec{k}$. For the Yukawa folding function of Eq. (34) one finds

$$\hat{g}(k) = \frac{1}{(2\pi)^{3/2}} \frac{1}{1 + a^2 k^2} \tag{39}$$

which then yields for the Coulomb potential V_c of Eq. (38)

$$V_c(\vec{r}_1) = \frac{e\rho_0}{i\pi a^2} \int_V d^3 r_3 \, \frac{1}{|\vec{r}_1 - \vec{r}_3|} \int_{-\infty}^{\infty} dk \frac{e^{i\vec{k}(\vec{r}_1 - \vec{r}_3)}}{k(k^2 + a^{-2})}. \tag{40}$$

The k-integration in the above equation can be evaluated by contour integration in the complex plane and the residue theorem, which then allows to write the Coulomb potential as the sum of two terms

$$V_c(\vec{r}_1) = V_c^{(sharp)}(\vec{r}_1) + \triangle V_c(\vec{r}_1), \tag{41}$$

where the first terms, that yields the dominant contribution, corresponds to the Coulomb potential of a sharp-surface density distribution

$$V_c^{(sharp)}(\vec{r}_1) = e \, \rho_0 \int_V \frac{d^3 r_2}{|\vec{r}_1 - \vec{r}_2|} \tag{42}$$

and where the corrective term, generated by the diffuse surface, is given by

$$\triangle V_c(\vec{r}_1) = -e \, \rho_0 \int_V d^3 r_2 \, \frac{e^{-|\vec{r}_1 - \vec{r}_2|/a}}{|\vec{r}_1 - \vec{r}_2|}. \tag{43}$$

Converting the volume integrals into surface integrals by the use of the Gauss–Ostrogradsky theorem, one obtains explicit expressions for $V_c^{(sharp)}(\vec{r}_1)$ and $\triangle V_c(\vec{r}_1)$ which, in addition, turn out to be more convenient for numerical integration by the Gauss–Legendre quadrature method used in the corresponding code

$$V_c^{(sharp)}(\vec{r}_1) = -\frac{\rho_0 e}{2} \oint_S [d\vec{S}_2 \cdot (\vec{r}_1 - \vec{r}_2)] \frac{1}{|\vec{r}_1 - \vec{r}_2|},$$

$$\begin{aligned} \triangle V_c(\vec{r}_1) = {}& \frac{\rho_0 e}{a} \oint_S [d\vec{S}_2 \cdot (\vec{r}_1 - \vec{r}_2)] \left(\frac{|\vec{r}_1 - \vec{r}_2|}{a}\right)^{-3} \\ &\times \left[1 - \left(1 + \frac{|\vec{r}_1 - \vec{r}_2|}{a}\right) e^{-\frac{|\vec{r}_1 - \vec{r}_2|}{a}}\right]. \end{aligned} \tag{44}$$

3.2. Mean-field nuclear potential

Since the mean-field potential in which the nucleons evolve and which is generated by their mutual interaction should have a shape that follows the one of the nucleon density distribution, one should be able to obtain these proton and neutron potentials by a convolution of the nuclear density with a Yukawa-like function. The latter can be considered here as a spin independent two-body interaction (interaction between two infinitesimal volume elements of a nuclear drop (see, e.g. Ref. [12]))

$$V_N(\vec{r}_1) = \int_V d^3 r_2 \, \tilde{v}(r_{12}) \, \frac{\rho(\vec{r}_2)}{\rho_0}, \tag{45}$$

where

$$\tilde{v}(r_{12}) = -\frac{V_0}{4\pi \lambda^3} \frac{e^{-|\vec{r}_1 - \vec{r}_2|/\lambda}}{|\vec{r}_1 - \vec{r}_2|/\lambda}, \qquad r_{12} = |\vec{r}_1 - \vec{r}_2|. \tag{46}$$

In general, one assumes that the range λ of the Yukawa interaction is slightly different from the range a of the folding function of the same type used to generate the diffuse density distribution in Eq. (31).

Proceeding in the same way as for the Coulomb potential, one obtains the nuclear part of the mean-field potential as the sum of two terms

$$V_N(\vec{r}_1) = V_N^{(sharp)}(\vec{r}_1) + \Delta V_N(\vec{r}_1). \tag{47}$$

Converting again the spatial integrals into surface integrals through the Gauss–Ostrogradsky theorem and remembering that the diffuseness parameters a and λ used to generate respectively the diffuse density and the nuclear mean-field potential are, in general different, one obtains with $\vec{r}_{12} \equiv \vec{r}_1 - \vec{r}_2$

$$V_N^{(sharp)}(\vec{r}_1) = \frac{V_0}{4\pi\lambda^3} \oint_S \left(d\vec{S}_2 \cdot \vec{r}_{12} \right) \left(\frac{|\vec{r}_1 - \vec{r}_2|}{\lambda} \right)^{-3}$$
$$\times \left[1 - \left(1 + \frac{|\vec{r}_1 - \vec{r}_2|}{\lambda} \right) e^{\frac{|\vec{r}_1 - \vec{r}_2|}{\lambda}} \right] \tag{48}$$

and

$$\Delta V_N(\vec{r}_1) = -\frac{a^2}{a^2 - \lambda^2} V_N^{(sharp)}(\vec{r}_1)$$
$$+ \oint_S \left(d\vec{S}_2 \cdot \vec{r}_{12} \right) \left(\frac{|\vec{r}_1 - \vec{r}_2|}{a} \right)^{-3}$$
$$\times \left[1 - \left(1 + \frac{|\vec{r}_1 - \vec{r}_2|}{a} \right) e^{\frac{|\vec{r}_1 - \vec{r}_2|}{a}} \right]. \tag{49}$$

In cylindrical coordinates (ρ, φ, z), the surface element $d\vec{S}$ can be written as

$$d\vec{S} = \sqrt{1 + \frac{1}{\rho^2} \left(\frac{\partial\rho}{\partial\varphi} \right)^2 + \left(\frac{\partial\rho}{\partial z} \right)^2} \, \rho \, dz \, d\varphi \, \vec{n}, \tag{50}$$

where $\vec{n}$ is the unit vector normal to the surface at a given point (ρ, φ, z)

$$\vec{n} = \frac{\left[1, -\frac{1}{\rho}\frac{\partial\rho}{\partial\varphi}, -\frac{\partial\rho}{\partial z} \right]}{\sqrt{1 + \frac{1}{\rho^2} \left(\frac{\partial\rho}{\partial\varphi} \right)^2 + \left(\frac{\partial\rho}{\partial z} \right)^2}}. \tag{51}$$

The last two equations lead to the following form for the vector surface element

$$d\vec{S} = \left[\rho, -\frac{\partial\rho}{\partial\varphi}, -\rho\frac{\partial\rho}{\partial z} \right] dz \, d\varphi, \tag{52}$$

where we have used the decomposition of the vector $d\vec{S}$ in the cylindrical coordinate basis vectors $\left[\vec{e}_\rho, \vec{e}_\varphi, \vec{e}_z \right]$.

The splitting of folded quantities like the Coulomb and the nuclear potential into a *sharp* and a *diffuse* component is mathematically strict, but, as was demonstrated in Ref. [12], not really necessary since the effect of the density diffuseness can be practically mocked up by a *renormalization* of the diffuseness parameter λ of the *sharp-density* contribution. In addition, the *diffuse-density* correction turns out to vary very slowly with the nuclear deformation. For these reasons the diffuseness corrections $\Delta V_c(\vec{r}_1)$ of Eq. (43) as well as $\Delta V_N(\vec{r}_1)$ of Eq. (49) are no longer taken into account in the numerical applications of the theory developed below.

The non-local spin–orbit component of the single-particle mean-field potential can be generated using the central part of the potential V_N, Eq. (45), in the standard way

$$V_{s.o.} = i W_{s.o.}^{(q)} \left(\frac{\hbar}{2Mc} \right)^2 \vec{\nabla} V_N \cdot \left[\vec{\sigma} \times \vec{\nabla} \right], \quad q = \{n, p\}, \tag{53}$$

where M is the nucleon mass and $\vec{\sigma}$ denotes the 2×2 Pauli matrices $(\sigma_x, \sigma_y, \sigma_z)$.

Table 1
Constants used in the Yukawa-folding procedure [6].

Constant	Value	Unit	Constant	Value	Unit
λ	0.8	[fm]	J	35.0	[MeV]
a	0.7	[fm]	Q	25.0	[MeV]
V_s	52.5	[MeV]	c_1	$\frac{3}{5}\frac{e^2}{r_0}$	[MeV]
V_a	48.7	[MeV]	M	938.9	[MeV/c^2]

Following Ref. [6] we have used the following parametrization of the depths of the central parts of the single-particle potentials for protons and neutrons:

$$V_0^p = V_s + V_a \, \bar{\delta},$$
$$V_0^n = V_s - V_a \, \bar{\delta}, \tag{54}$$

where

$$\bar{\delta} = \left(I + \frac{3}{8}\frac{c_1}{Q}\frac{Z^2}{A^{5/3}} \right) \bigg/ \left(1 + \frac{9}{4}\frac{J}{Q}\frac{1}{A^{1/3}} \right), \quad I = \frac{N - Z}{A} \tag{55}$$

where c_1, Q and J are the droplet model constants widely discussed e.g. in [6]. Quantities V_s and V_a that are called symmetric and asymmetric potential-depth constants by the authors of Ref. [6] are determined from considerations other than nuclear masses (for more details, see [6] and references therein). Please also note that the strength parameter $W_{s.o.}$ of the spin–orbit field which according to Eq. (53) is a dimensionless quantity has to be chosen slightly differently for protons and neutrons. According to Ref. [6] we take

$$W_{s.o.}^{(p)} = 6.0 \left(\frac{A}{240} \right) + 28.0 \quad \text{and}$$

$$W_{s.o.}^{(n)} = 4.5 \left(\frac{A}{240} \right) + 31.5. \tag{56}$$

Recall that the model constants a and λ describe the range of the Yukawa function used to generate the nuclear charge distribution (not further used in the following calculations) and the central potential, respectively. The parameter λ and the spin–orbit parameters of Eq. (56) have been determined from an adjustment of calculated single-particle levels to experimental data for the rare-earth and actinide nuclei for details see references in [6]. All parameters used in the calculations are collected in Table 1.

At the end of our discussion of folded potentials, let us compare in Fig. 4 the form of the Yukawa-folded potentials with the corresponding Woods–Saxon potential obtained with the so-called universal set of parameters [14] for nuclei in different regions of the periodic table, namely actinide, rare-earth and light nuclei (^{240}Pu, ^{156}Gd and ^{56}Fe) always imposing spherical symmetry. One notices that the Yukawa-folded mean field, Eq. (48), and the Woods–Saxon central potentials are very close to each other. A slight difference of ≈ 0.5 MeV is observed in the depths of the proton and neutron wells of Pu and Gd nuclei and of about ≈ 1.5 MeV in Fe.

4. Diagonalization of a triaxial mean-field potential in a harmonic oscillator basis

The knowledge of the single-particle energies and wave-functions of an atomic nucleus is the starting point to various nuclear-structure investigations. For the description of the average single-particle field in the absence of spherical or axial symmetry the Cartesian coordinate system seems to be the most suitable. In this case all three coordinates are treated on the same footing and, in principle, no symmetry conditions are imposed on the basis wave-functions. Of course, in such a coordinate system the angular
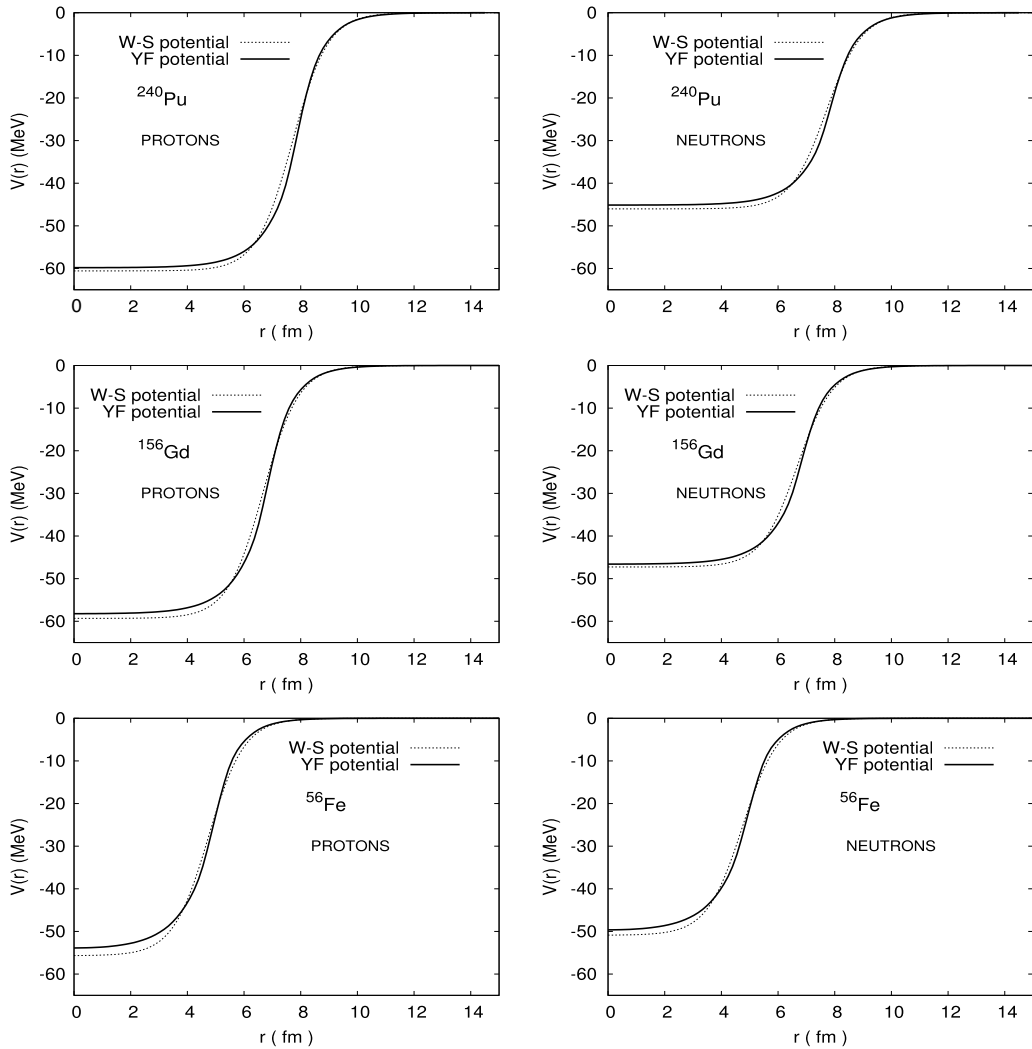
Fig. 4. Comparison of the spherical Yukawa-folded (solid line) and Woods–Saxon (dashed line) nuclear potentials of ^{240}Pu (top), ^{156}Gd (middle) and ^{56}Fe (bottom) isotopes for protons (l.h.s.) and for neutrons (r.h.s.)

momentum algebra cannot be applied directly to the resulting wave functions even if the symmetry of the system turns out to be accidentally spherical or axial. In the following we present the expressions for the matrix elements of all components of the total single-particle Hamiltonian. Recall that the Hamiltonian matrix is, in general, Hermitian and, through an adequate choice of phase factors, real.

4.1. Construction of the harmonic-oscillator basis states

To simplify the calculation in the absence of the above mentioned symmetries, one generally uses the well-known eigenfunctions of a triaxial harmonic oscillator Hamiltonian as the basis in which the eigenfunctions of any given mean-field potential can then be developed, i.e. one starts from

$$\hat{\mathcal{H}}_{h.o.} = \frac{-\hbar^2}{2m}\hat{\Delta} + \frac{m}{2}\left(\omega_x^2 x^2 + \omega_y^2 y^2 + \omega_z^2 z^2\right), \qquad (57)$$

where the ω_i, $i = \{x, y, z\}$ are the oscillator frequencies in the three Cartesian directions. Its eigenvalues are given as

$$E(n_x, n_y, n_z) = \hbar\omega_x\left(n_x + \frac{1}{2}\right) + \hbar\omega_y\left(n_y + \frac{1}{2}\right)$$

$$+ \hbar\omega_z\left(n_z + \frac{1}{2}\right) \qquad (58)$$

and the corresponding normalized harmonic-oscillator eigenstates as

$$|n_x, n_y, n_z, \Sigma\rangle \equiv i^{n_y}\Psi_{n_x}(x)\Psi_{n_y}(y)\Psi_{n_z}(z)\chi(\Sigma)$$

$$= i^{n_y}\sqrt{a_x a_y a_z}\, H_{n_x}(\xi)H_{n_y}(\eta)H_{n_z}(\zeta)\chi(\Sigma)e^{-\frac{1}{2}(\xi^2 + \eta^2 + \zeta^2)}, \qquad (59)$$

where $\chi(\Sigma)$ is the spinor with two possible choices only, corresponding to spin up or down orientation ($\chi(\Sigma) = |\uparrow\rangle$ or $\chi(\Sigma) = |\downarrow\rangle$). Here H_n is the nth order normalized Hermite polynomial

$$H_n(u) = \sqrt{\frac{1}{\sqrt{\pi}2^n n!}}\tilde{H}_n(u), \qquad (60)$$

where the non-normalized Hermite polynomial $\tilde{H}_n(u)$ can be obtained through

$$\tilde{H}_n(u) = (-1)^n e^{u^2}\frac{d^n}{du^n}e^{-u^2}, \quad n = 0, 1, 2, \ldots \qquad (61)$$

The phase factor i^{n_y} in (59) is chosen to ensure the Yukawa mean-field Hamiltonian matrix elements to be real numbers.

One can define characteristic lengths

$$a_i = \sqrt{\frac{M\omega_i}{\hbar}} \qquad (62)$$

in each of the three Cartesian directions which then allow to define dimensionless variables

$$\xi \equiv a_1 x, \qquad \eta \equiv a_2 y, \qquad \zeta \equiv a_3 z \tag{63}$$

on which the Hermite polynomial in Eq. (59) depend. The three oscillator constants ω_i can, however, not be chosen arbitrarily, but are related by the fact that the volume of the equipotential harmonic oscillator surface does not change with deformation. In addition, the ratios ω_x/ω_z and ω_y/ω_z are chosen in such a way that the surface of the deformed nucleus and the equipotential harmonic oscillator surface are as close as possible. Calling ω_0 the oscillator frequency corresponding to the spherical shape, one has

$$\omega_x \omega_y \omega_z = \omega_0^3, \tag{64}$$

where in numerical application a value of $\hbar\omega_0 = 41$ MeV/A$^{1/3}$ is generally used. This corresponds roughly to the energy spacing between major shells in the harmonic oscillator spectrum.

Let us in the following recall a certain number of properties of the above defined Hermite polynomials which we have used to evaluate the different types of matrix elements in our computer code:

$$\tilde{H}_{n+1}(u) = 2u\tilde{H}_n(u) - 2n\tilde{H}_{n-1}(u), \tag{65}$$

$$\frac{d}{du}\tilde{H}_n(u) = 2n\tilde{H}_{n-1}(u). \tag{66}$$

Multiplying both sides of Eq. (65) by $\tilde{H}_{n'}(u)$ one obtains

$$\tilde{H}_{n+1}(u)\,\tilde{H}_{n'}(u) = 2u\tilde{H}_n(u)\,\tilde{H}_{n'}(u) - 2n\tilde{H}_{n-1}(u)\,\tilde{H}_{n'}(u). \tag{67}$$

In order to eliminate the undesired factor $2u\tilde{H}_{n'}(u)$ on the right-hand side of this equation we apply again Eq. (65) with index n replaced by n'

$$2u\tilde{H}_{n'}(u) = \tilde{H}_{n'+1}(u) + 2n'\,\tilde{H}_{n'-1}(u). \tag{68}$$

Introducing the normalization of Hermite polynomials $\tilde{H}$ and substituting $n \to n'' - 1$ in Eq. (67) one finally obtains

$$H_{n''}H_{n'} = \sqrt{\frac{n'+1}{n''}}H_{n''-1}H_{n'+1} + \sqrt{\frac{n'}{n''}}H_{n''-1}H_{n'-1} - \sqrt{\frac{n''-1}{n''}}H_{n''-2}H_{n'}. \tag{69}$$

Another very useful property of normalized Hermite polynomials (60) is their orthogonality relation

$$\int_{-\infty}^{\infty} H_n(u)\,H_{n'}(u)\,e^{-u^2}\,du = \delta_{nn'}. \tag{70}$$

Matrix elements of the one-body kinetic-energy operator

$$T_{kin} = T_{kin}^{(xyz)} + T_{kin}^{(zxy)} + T_{kin}^{(yzx)} \tag{71}$$

in the basis of the triaxial h.o. potential can be easily derived analytically between states of the same spin projections Σ with the help of relations (65)–(70):

$$\langle n_x', n_y', n_z', \Sigma' \mid T_{kin}^{(xyz)} \mid n_x, n_y, n_z, \Sigma \rangle$$
$$= \delta_{\Sigma'\Sigma}\left\{\hbar\omega_z\left[\frac{1}{2}\left(n_z + \frac{1}{2}\right)\delta_{n_z n_z'} - \frac{1}{4}\sqrt{n_z(n_z-1)}\,\delta_{n_z-2,n_z'}\right.\right.$$
$$\left.\left. - \frac{1}{4}\sqrt{n_z'(n_z'-1)}\,\delta_{n_z,n_z'-2}\right]\delta_{n_x n_x'}\,\delta_{n_y n_y'}\right\}, \tag{72}$$

where the matrix elements of the other two terms in (71) are calculated by cyclical variation of indices (x, y, z) in Eq. (72), i.e. $(x, y, z) \to (z, x, y) \to (y, z, x)$.

Let us now calculate the matrix elements of the local mean-field potential V_{sp} which can be any local potential (V_N, Eq. (45), or V_c, Eq. (36)), of arbitrary shape

$$\langle n_x', n_y', n_z', \Sigma' \mid V_{sp} \mid n_x, n_y, n_z, \Sigma \rangle$$
$$= \langle n_x', n_y', n_z' \mid V_{sp} \mid n_x, n_y, n_z \rangle\,\delta_{\Sigma'\Sigma}, \tag{73}$$

where

$$\langle n_x', n_y', n_z' \mid V_{sp} \mid n_x, n_y, n_z \rangle$$
$$= i^{(n_y'-n_y)} \int_{-\infty}^{\infty} d\xi\, e^{-\xi^2}\, H_{n_x'}(\xi)\, H_{n_x}(\xi) \cdot$$
$$\times \int_{-\infty}^{\infty} d\eta\, e^{-\eta^2}\, H_{n_y'}(\eta)\, H_{n_y}(\eta)$$
$$\cdot \int_{-\infty}^{\infty} d\zeta\, e^{-\zeta^2}\, H_{n_z'}(\zeta)\, H_{n_z}(\zeta)\, V(\xi, \eta, \zeta). \tag{74}$$

The largest part of the above matrix elements can be calculated recursively by virtue of the relation (69) and using the orthogonality relation (70). The matrix elements of the single-particle potential V_{sp} can then be rewritten as

$$\langle n_x', n_y', n_z' \mid V_{sp} \mid n_x, n_y, n_z \rangle$$
$$= \sqrt{\frac{n_z'+1}{n_z}}\,\langle n_x', n_y', n_z'+1 \mid V_{sp} \mid n_x, n_y, n_z-1 \rangle$$
$$+ \sqrt{\frac{n_z'}{n_z}}\,\langle n_x', n_y', n_z'-1 \mid V_{sp} \mid n_x, n_y, n_z-1 \rangle$$
$$- \sqrt{\frac{n_z-1}{n_z}}\,\langle n_x', n_y', n_z' \mid V_{sp} \mid n_x, n_y, n_z-2 \rangle. \tag{75}$$

Similar relations can be derived for recursion in the x and y direction.

In the code one can immediately identify, simply by studying the parity of the integrand in Eq. (74), the matrix elements which are, by the parity symmetry conditions, equal to zero. As an example let us take a potential which is symmetric with respect to the z-axis (not necessarily strictly axially symmetric). As a consequence, a certain number of matrix elements vanish due to the fact that V_{sp} in Eq. (74) is then an even function in x-direction ($V(x, y, z) = V(-x, y, z)$) and one obtains a zero result if the sum of quantum numbers ($n_x' + n_x$) of the basis states turns out to be an odd number. A similar reasoning can be applied to the two other (y and z) directions.

Let us now come to the description of the term in the Hamiltonian which couples the spin and the orbital motion in the quantum system, referred to as the spin–orbit potential. This potential, as given in Eq. (53) for the two nucleon charge states (n and p), can be obtained from the respective nuclear central potential, so that this potential can be rewritten, after obvious algebraic transformations, as a linear combination of products involving spatial and spin operators in the following form:

$$V_{s.o.} = i\,W_{s.o.}\left(\frac{\hbar}{2Mc}\right)^2\left[\hat{\sigma}_x\left(\frac{\partial V_{sp}}{\partial z}\partial_y - \frac{\partial V_{sp}}{\partial y}\partial_z\right)\right.$$
$$\left. + \hat{\sigma}_y\left(\frac{\partial V_{sp}}{\partial x}\partial_z - \frac{\partial V_{sp}}{\partial z}\partial_x\right) + \hat{\sigma}_z\left(\frac{\partial V_{sp}}{\partial y}\partial_x - \frac{\partial V_{sp}}{\partial x}\partial_y\right)\right]. \tag{76}$$

Keeping in mind that the spin–orbit potential is different for protons and neutrons (see, Eq. (53)), the charge index q is omitted

in what follows and one can simply write

$$\langle n'_x, n'_y, n'_z, \Sigma' \mid V_{s.o.} \mid n_x, n_y, n_z, \Sigma \rangle = i\, W_{s.o.} \left(\frac{\hbar}{2Mc}\right)^2$$

$$\cdot \left\{ \langle n'_x, n'_y, n'_z, \Sigma' | \hat{\sigma}_x \left(\frac{\partial V_{sp}}{\partial z}\,\partial_y - \frac{\partial V_{sp}}{\partial y}\,\partial_z\right) | n_x, n_y, n_z, \Sigma \rangle \right.$$

$$+ \langle n'_x, n'_y, n'_z, \Sigma' \mid \hat{\sigma}_y \left(\frac{\partial V_{sp}}{\partial x}\,\partial_z - \frac{\partial V_{sp}}{\partial z}\,\partial_x\right) \mid n_x, n_y, n_z, \Sigma \rangle$$

$$\left. + \langle n'_x, n'_y, n'_z, \Sigma' | \hat{\sigma}_z \left(\frac{\partial V_{sp}}{\partial y}\,\partial_x - \frac{\partial V_{sp}}{\partial x}\,\partial_y\right) | n_x, n_y, n_z, \Sigma \rangle \right\}. \quad (77)$$

For further applications it is convenient to express the Cartesian spin operators $\{\hat{\sigma}_x, \hat{\sigma}_y, \hat{\sigma}_z\}$ in terms of the ladder operators

$$\hat{\sigma}_+ = (\hat{\sigma}_x + i\hat{\sigma}_y), \qquad \hat{\sigma}_- = (\hat{\sigma}_x - i\hat{\sigma}_y), \qquad \hat{\sigma}_0 = \hat{\sigma}_z, \quad (78)$$

which act on the spin part of the general wave function in the following way:

$$\hat{\sigma}_+ |\downarrow\rangle = |\uparrow\rangle, \qquad \hat{\sigma}_- |\downarrow\rangle = 0, \qquad \hat{\sigma}_z |\downarrow\rangle = |\downarrow\rangle,$$

$$\hat{\sigma}_+ |\uparrow\rangle = 0, \qquad \hat{\sigma}_- |\uparrow\rangle = |\downarrow\rangle, \qquad \hat{\sigma}_z |\uparrow\rangle = |\uparrow\rangle. \quad (79)$$

Since the partial derivatives of an arbitrary local potential, that appear in (77), can, in the general case, not be determined analytically, it is convenient to perform in (77) an integration by parts that generates some partial derivatives of the basis wave functions. Keeping in mind that these wave functions $\Psi_n(u)$ vanish at infinity, one finds together with the explicit form of the derivative of the Ψ_n relations like

$$\frac{d\Psi_{n_x}(a_x x)}{dx} = \mathcal{N}_{n_x}\sqrt{a_x}\left(a_x H'_{n_x-1}(a_x x) - a_x^2\, x\, H_{n_x}(a_x x)\right) e^{-\frac{1}{2}a_x^2 x^2}$$

$$= a_x\left[\sqrt{\frac{n_x}{2}}\,\Psi_{n_x-1}(x) - \sqrt{\frac{n_x+1}{2}}\,\Psi_{n_x+1}(x)\right] \quad (80)$$

which yields

$$\langle n'_x, n'_y, n'_z, \Sigma' \mid V_{s.o.} \mid n_x, n_y, n_z, \Sigma \rangle$$

$$= \frac{i}{2}\, W_{s.o.} \left(\frac{\hbar}{2Mc}\right)^2 \left[\langle \Sigma' | \sigma_+ | \Sigma \rangle B_-\right.$$

$$\left. + \langle \Sigma' | \sigma_- | \Sigma \rangle B_+ + 2\langle \Sigma' | \sigma_z | \Sigma \rangle B_z\right], \quad (81)$$

where

$$B_\pm \equiv B_x \mp B_y, \quad (82)$$

with

$$B_x = \frac{1}{2}\left[1 - (-1)^{n'_y+n_y}\right] a_y a_z$$

$$\times \left\{-\sqrt{n'_z(n_y+1)}\langle n'_x, n'_y, n'_z-1, |V_{sp}|n_x, n_y+1, n_z\rangle\right.$$

$$-\sqrt{n_y(n'_z+1)}\langle n'_x, n'_y, n'_z+1, |V_{sp}|n_x, n_y-1, n_z\rangle$$

$$+\sqrt{n'_y(n_z+1)}\langle n'_x, n'_y-1, n'_z, |V_{sp}|n_x, n_y, n_z+1\rangle$$

$$\left. +\sqrt{n_z(n'_y+1)}\langle n'_x, n'_y+1, n'_z, |V_{sp}|n_x, n_y, n_z-1\rangle\right\},$$

$$B_y = \frac{1}{2}\left[1 + (-1)^{n'_y+n_y}\right] a_x a_z$$

$$\times \left\{-\sqrt{n'_x(n_z+1)}\langle n'_x-1, n'_y, n'_z, |V_{sp}|n_x, n_y, n_z+1\rangle\right.$$

$$-\sqrt{n_z(n'_x+1)}\langle n'_x+1, n'_y, n'_z, |V_{sp}|n_x, n_y, n_z-1\rangle$$

$$+\sqrt{n'_z(n_x+1)}\langle n'_x, n'_y, n'_z-1, |V_{sp}|n_x+1, n_y, n_z\rangle$$

$$\left. +\sqrt{n_x(n'_z+1)}\langle n'_x, n'_y, n'_z+1, |V_{sp}|n_x-1, n_y, n_z\rangle\right\}, \quad (83)$$

$$B_z = \frac{1}{2}\left[1 - (-1)^{n'_y+n_y}\right] a_x a_y$$

$$\times \left\{-\sqrt{n'_y(n_x+1)}\langle n'_x, n'_y-1, n'_z, |V_{sp}|n_x+1, n_y, n_z\rangle\right.$$

$$-\sqrt{n_x(n'_y+1)}\langle n'_x, n'_y+1, n'_z, |V_{sp}|n_x-1, n_y, n_z\rangle$$

$$+\sqrt{n'_x(n_y+1)}\langle n'_x-1, n'_y, n'_z, |V_{sp}|n_x, n_y+1, n_z\rangle$$

$$\left. +\sqrt{n_y(n'_x+1)}\langle n'_x+1, n'_y, n'_z, |V_{sp}|n_x, n_y-1, n_z\rangle\right\}.$$

As one can see from Eq. (81), the terms in the spin–orbit interaction, that are proportional to B_- and B_+, couple only *antiparallel* spin states, whereas those containing B_z acts between states of *parallel* spin orientation. This is different from the case of the central potential which gives non zero contributions only between states of the same spin projection. This unique feature of the spin–orbit potential leads to the well-known energy splitting of each single-particle level (except for s-states) into two levels of the same orbital angular momentum but opposite spin orientations.

In order to build the full matrix of the central potential recursively it is enough to calculate numerically all diagonal matrix elements, as well as a few of those off-diagonal matrix elements which, for certain combinations of $\{n_x, n_y, n_z\}$, cannot be determined by recursion. The number of such elements adds up to only a few percent of the total. The rest of the off-diagonal matrix elements are determined in successive, parallel lines to the main diagonal of the matrix. After the computation of the average-potential matrix elements, one has to do the same for the spin–orbit potential with the help of the relation (81).

It is also possible to calculate them purely recursively under the condition that one first calculates a few additional matrix elements of the central potential for which $n_x + n_y + n_z = N_{max} + 1$, (where N_{max} denotes the cut-off condition referring to the number of spherical oscillator main shells used in the expansion of the total wave function).

4.2. Matrix representation of the mean-field Hamiltonian in the case of z-signature symmetry

Let us recall that the formalism presented in the previous subsection is valid for an arbitrary potentials without imposing any additional spatial symmetry, only requiring time-reversal symmetry.

Let us now restrict the class of nuclear shapes to those characterized by the so-called *z-signature* symmetry, $\hat{R}_z$, corresponding to a rotation by an angle π about the z-axis. Requiring the invariance of the potential $V(x, y, z)$ with respect to the $\hat{R}_z$ operation, one obtains

$$V(x, y, z) = V(-x, -y, z). \quad (84)$$

The two above presented shape parametrizations, the Funny–Hills and the Trentalange–Koonin–Sierk shapes (see Sections 2.1 and 2.2) have in the case of a spheroidal section perpendicular to the z-axis (see Section 2.4) exactly this symmetry. One could, of course, imagine a vast variety of other geometrical shapes for which the condition (84) is also valid.

The action of $\hat{R}_z$ on spin states $|s = \frac{1}{2}, \Sigma = \frac{1}{2}\rangle \equiv |+\rangle$ and $|s = \frac{1}{2}, \Sigma = -\frac{1}{2}\rangle \equiv |-\rangle$ yields

$$e^{-i\pi\Sigma/\hbar}|+\rangle = (-i)|+\rangle, \qquad e^{-i\pi\Sigma/\hbar}|-\rangle = (+i)|-\rangle. \quad (85)$$

The quantum number associated with this symmetry, can therefore be given in the simplified form as [15]

$$r_z = (-1)^{n_x+n_y}\,\frac{\Sigma}{|\Sigma|}, \quad (86)$$

where Σ is the projection $\{1/2, -1/2\}$ of the spin onto the quantization z-axis. Notice that we do not impose any limitations concerning the symmetry of the shape in z-direction. Then r_z given by (86) as the only good quantum number of our eigenvalue problem, splits the Hamiltonian matrix into two identical blocks with $r_z = 1$ and $r_z = -1$, respectively.

Hence, it will be sufficient to diagonalize only one of these blocks and, according to the Kramer's theorem, every state can then be occupied by two particles. We can therefore conclude that the here discussed symmetry transformation contains already the time reversal operation. Schematically the Hamiltonian matrix may be presented as (with e.g. $|b_{odd} \uparrow\rangle$ denoting the basis state (59) for which $n_x + n_y$ is an odd number with spin projection $+1/2$, marked symbolically by $|\uparrow\rangle$):

$$
\begin{pmatrix}
|b_{odd}\,\uparrow\rangle & |b_{even}\,\downarrow\rangle & |b_{odd}\,\downarrow\rangle & |b_{even}\,\uparrow\rangle \\
V_{cent}+V_{s.o.;3} & V_{s.o.1}+V_{s.o.;2} & 0 & 0 \\
V_{s.o.1}-V_{s.o.;2} & V_{cent}-V_{s.o.;3} & 0 & 0 \\
0 & 0 & V_{cent}+V_{s.o.;3} & V_{s.o.,1}+V_{s.o.;2} \\
0 & 0 & V_{s.o.;1}-V_{s.o.;2} & V_{cent}-V_{s.o.;3}
\end{pmatrix}
\begin{matrix}
|b_{odd}\,\uparrow\rangle \\
|b_{even}\,\downarrow\rangle \\
|b_{odd}\,\downarrow\rangle \\
|b_{even}\,\uparrow\rangle
\end{matrix}
$$

By analogy, the meaning of the three other types of basis states is obvious. The quantities V_{centr} and $V_{s.o.;\nu}$ are given respectively by $V_{centr} = V_{kin} + V_N$ for neutrons and $V_{centr} = V_{kin} + V_N + V_{Coul}$ for protons, while $V_{s.o.;\nu}, (\nu = \{1, 2, 3\})$ corresponds to the spin–orbit term, entering Eq. (81), proportional respectively to B_x, B_y, B_z. Keeping in mind the above reasoning, we conclude that the upper-left and the lower-right blocks of the full matrix must be identical, i.e. must have the same eigensolutions.

4.3. Numerical accuracy of the calculations

The primary source of error in calculating the single-particle energies and wave functions is the truncation of the harmonic oscillator basis expressed in terms of the maximum number N_{max} (or NMAX as used in the code) of oscillator shells taken into account. Integration errors involved in the calculation of the matrix elements, folding of the potential and diagonalization of the Hamiltonian matrix can, in practice, be made negligibly small as compared to this truncation error.

The strongly bound single-particle state, lying close to the bottom of the potential well, converges for NMAX $\geq$ 14 oscillator shells within the whole deformation range, as shown in the bottom part of Fig. 5, whereas the state lying substantially above the Fermi surface converges only for NMAX $\geq$ 18 shells (note that in numbering of single-particle states the two-fold Kramer's degeneracy is taken into account).

We can state therefore that the unbound levels from the energy-continuum approach to zero energy as the basis becomes infinite. This statement is true since we know that **any** positive energy is a solution of the Schrödinger equation. In order to simulate the energy continuum the density of the unbound levels must approaches infinity what is possible only when the basis is going to be infinitely large. Thus, levels calculated with a finite basis **do not** represent strictly speaking any physical resonant states. Nevertheless, they are often used to calculate the microscopic (shell and pairing) energy corrections which require the knowledge of levels, also above the Fermi level.

Since for practical applications an upper limit of the number of oscillator basis states is required, we introduce a so called "*energy cut-off*" parameter E_{cutoff} expressed in terms of the average
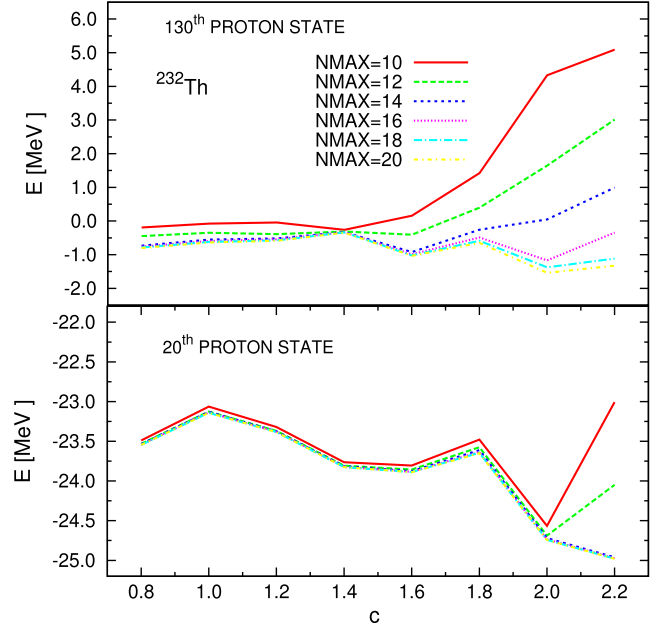
Fig. 5. Convergence of a loosely bound proton state as function of the deformation parameter c and the oscillator shell number NMAX in a ^{232}Th nucleus (top) and for a strongly bound proton state (bottom).

distance between major oscillator shells $\Delta E_{shell} = \hbar\omega_0$, and the energy of the last effective oscillator shell numbered by N_{cutoff} (or NCUT in the code). Both these quantities are related by

$$
E_{cutoff} = N_{cutoff}\,\hbar\omega_0 = N_{cutoff}\,\hbar(\omega_x \omega_y \omega_z)^{1/3}, \tag{87}
$$

where $\omega_i, i = \{x, y, z\}$ are the respective oscillator frequencies in x, y and z direction of Eq. (64) and ω_0 denotes the frequency of the corresponding spherical oscillator as explained in the previous section. The quantities ω_i, determined in the subroutine OMEGAS, called by the YUKA subprogram, play the role of the basis parameters.

In connection with the cut-off energy, one introduces another important parameter NMAX which is part of the PARAMETER statement of the three subroutines YUKA, VTOTAL and RNEWMA. This quantity corresponds to the number of the highest **spherical** oscillator shell included in the calculation, thus determining the maximal total number of basis states NDEG that are taken into account. That number, determined by NMAX, neglecting the Kramer's degeneracy is given as

$$
\text{NDEG(NMAX)} = \frac{1}{6}(\text{NMAX}+1)(\text{NMAX}+2)(\text{NMAX}+3). \tag{88}
$$

The test choice made in our computer code is NMAX = 14 and corresponds to NDEG(14) = 680 basis states. The quantity NDEG represents the *maximal* number of basis states, taking into account the fact that this number can still be reduced since a certain number of these states might have energies *beyond* the cut-off energy introduced in Eq. (87) and will therefore not be taken into account in the calculation. As seen in Table 2, the actual number NDIAG of basis states that are really included in the calculation is evidently, due to the cut-off condition, smaller or equal to NDEG. It is clear that the number of such "out-of-bounds" states increases with increasing NMAX. On the contrary, some basis states corresponding to higher oscillator shells might have their energy come down substantially with increasing deformation and one has to be very cautious, not to artificially eliminate physically relevant basis states by a too small choice of NMAX.

For a given nuclear deformation, one can decide, according to the energy of the eigenstate, Eq. (58), about the order of the

Table 2
Dimension of the basis NDIAG as function of oscillator shell number NMAX and deformation parameter c.

c	Dimension of the basis NDIAG					
	NMAX = 10	NMAX = 12	NMAX = 14	NMAX = 16	NMAX = 18	NMAX = 20
0.8	286	455	680	968	1262	1462
1.0	286	455	680	969	1292	1534
1.2	286	455	680	959	1248	1492
1.4	286	455	679	939	1195	1408
1.6	286	455	673	912	1141	1328
1.8	286	455	664	886	1093	1264
2.0	286	453	649	847	1025	1174
2.2	286	448	632	813	973	1112

harmonic-oscillator eigenstates, which are defined through the set of quantum numbers $\{n_x, n_y, n_z\}$. Arranging these basis states by increasing energy, one defines arrays NX(n), NY(n), NZ(n) of dimension NDIAG that attribute to the nth oscillator eigenstate the corresponding quantum numbers, until the total number NDEG of basis states is reached, i.e. such that for all states that are included in the diagonalization $n_x + n_y + n_z \leq$ NMAX + 1. It could now very well happen, in particular for very large deformations, that, due to the values of the oscillator constants ω_x, ω_y, ω_z some basis states do not longer fulfil the cut-off condition (87), and should therefore not be included in the list of basis states that are used to diagonalize the mean-field Hamiltonian. On the other hand, some of these states are needed for a complete construction of all of the matrix elements, via the recurrence relations given in Section 4.1. That is why a second ensemble of arrays NXR(n), NYR(n), NZR(n) is defined that, in contrast to the above mentioned fields NX(n), NY(n), NZ(n), do not contain those basis states that fail to fulfil the cut-off condition (87). It is therefore the single-particle states defined by the quantum numbers NXR(n), NYR(n), NZR(n) that define the basis in which the diagonalization of the Hamiltonian matrix is carried out.

It is obvious from what has been said above that the resulting eigensolutions of our problem are becoming practically independent on the specific choice of the oscillator frequencies ω_i if NMAX is chosen larger and larger. It is, indeed, clear that for NMAX $\rightarrow \infty$, this basis is going to be complete for *any* choice of the ω_i. Thus one will be able to expand *any eigenstate* in that basis. We have, however, concluded studying Fig. 6 that to obtain an acceptable convergence of the eigensolutions within a wide range of the here considered quadrupole, octupole and hexadecapole deformations, e.g. from oblate, through prolate shapes up to the scission configurations, the number of oscillator shells for the states around the Fermi surface should be chosen at least NMAX = 14. For the heaviest elements, where the number of occupied single-particle states is getting still larger, one might have to further increase NMAX. Please, keep in mind that the diagonalization time is crudely proportional to the third power of NDIAG, the solution of the eigenvalue problem takes, depending of course on the algorithm used, about one order of magnitude of computing time more for NMAX = 20 than it does for NMAX = 14.

Once the basis states are prepared, the nuclear and the Coulomb potentials are calculated through the subroutine POTENTIAL and stored at the Gauss–Hermite (GH) mesh points $x_i^{(GH)}$ determined, together with the corresponding weights $w_i^{(GH)}$ as function of the number N_{GH} of Gauss–Hermite integration points by the subroutine GAUHER. Let us recall here that the Gauss–Hermite quadrature approximates the integral of any integrable function $f(x)$ on the interval $(-\infty, +\infty)$ in the following form

$$\int_{-\infty}^{+\infty} f(x)e^{-x^2} dx \approx \sum_{i=1}^{N_{GH}} w_i^{(GH)} f(x_i^{(GH)}). \tag{89}$$

It should be noted that the Gaussian factor of the basis function (59), does not appear explicitly in the code, but is already contained in the used Gauss–Hermite quadrature weights $\{w^{(GH)}\}$. Let us insist here on the fact that the number of Gauss–Hermite integration points N_{GH} needs to be sufficiently large to obtain an acceptable accuracy of the calculated integrals. In Fig. 7 the convergence of the four proton and neutron single-particle states close to Fermi surface is shown as a function of the number of Gauss–Hermite integration nodes N_{GH} and the nuclear elongation c.

Taking into account that the GH quadrature of order N_{GH} is able to calculate accurately the integral of any polynomial of order $2N_{GH} + 1$ with a Gaussian fall-off, one can conclude that the knowledge of a minimal number of 2NMAX $+ \Delta N_{GH}$ mesh points is required. Here NMAX refers to the highest order of a Hermite polynomial appearing in the product basis state (59) in any of the three Cartesian directions. The fact that the central potential appearing in the matrix elements (74) is almost flat in the interior region that extends over 3.5–5 fm in light and 5–7 fm in heavy nuclei and then goes rapidly to zero over a distance of approximately 1 fm as seen in Fig. 4, such a behaviour is practically impossible to describe by a combination of low-order Hermite polynomials. We therefore conclude studying Fig. 7 that ΔN_{GH} needs to be sufficiently large. For all studied nuclei, in particular for heavy nuclei, like those in the actinide region, with deformations extending over the whole range $0.8 \leq c \leq 2.0$, reliable results can be obtained with $\Delta N_{GH} \approx 12$.

Notice that, in contrast to the well-known phenomenological mean-field in the form of, e.g. Nilsson potential, which can be easily determined analytically, the Yukawa-folded potential is defined, in general, by a triple spatial integral over the product of a nuclear density and the Yukawa-folding functions (see, Eq. (45)). For such a form of a volume integral, the Gauss–Ostrogradsky theorem can be applied in order to transform the volume into a two-dimensional surface integral. In our computer code such two-dimensional integrals with finite lower and upper boundaries, x_l and x_u respectively, are solved numerically by means of a standard Gauss–Legendre (GL) quadrature, with N_{GL} mesh point, which for an arbitrary integrable function $g(x)$ can be written as

$$\int_{x_l}^{x_u} g(x) dx \approx \sum_{i=1}^{N_{GL}} w_i^{(GL)} g(x_i^{(GL)}), \tag{90}$$

where $x_i^{(GL)}$ are the GL mesh points and $w_i^{(GL)}$ the corresponding weights supplied by the subroutine GAULEG.

Finally, it is worth mentioning that a minor numerical problem appears while integrating terms that include $|\vec{r}_1 - \vec{r}_2|$ expression, as it shows up both in the Coulomb (44) and in the Yukawa-folded potential (45). In the case when $\vec{r}_1$ is close to $\vec{r}_2$, the expression $|\vec{r}_1 - \vec{r}_2|$ has a kind of *kink* which is practically impossible to reproduce, within the Gauss–Legendre quadrature method (90), by a linear combination of Legendre polynomial of reasonably low order. To avoid numerical inaccuracy associated with that problem,
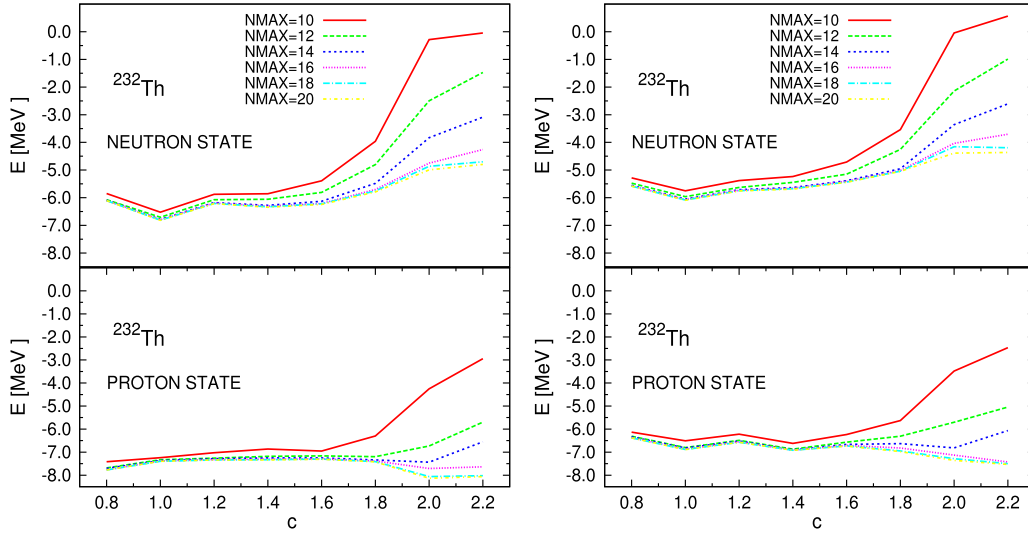
Fig. 6. Behaviour of neutron $(N_f^{(n)} - 2)$th (l.h.s. top) and proton $(N_f^{(p)} - 2)$th (l.h.s. bottom) single particle states in ^{232}Th isotope as function of deformation parameter c and oscillator shell number NMAX with the use of $N_{GH} = 48$ GH integration nodes. The same is shown for neutron $(N_f^{(n)} + 2)$th and proton $(N_f^{(p)} + 2)$th states in the r.h.s. top and bottom panels. Quantities $N_f^{(n)}$ and $N_f^{(p)}$ correspond respectively to $(A - Z)$th and Zth neutron and proton single-particle state.
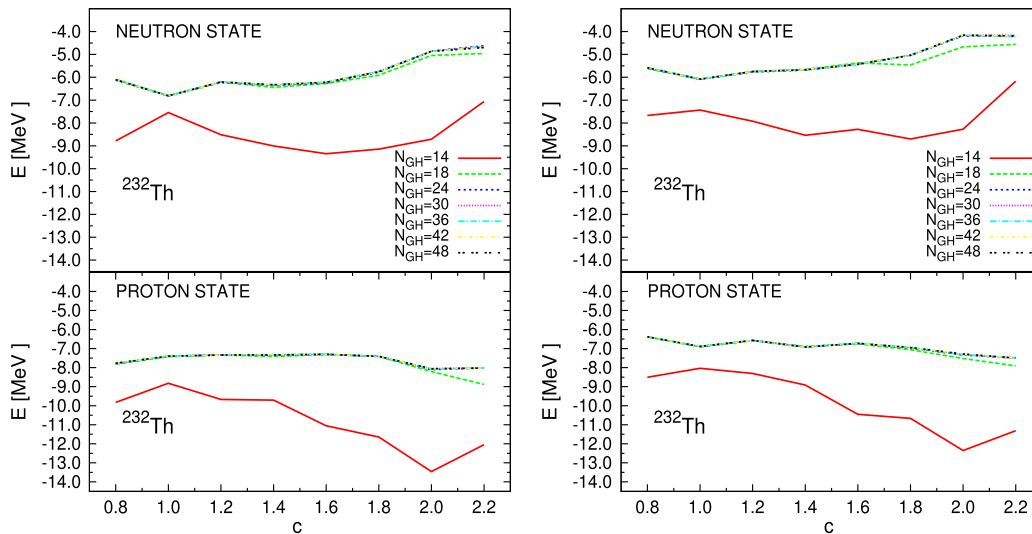
Fig. 7. Accuracy of determination of neutron $(N_f^{(n)} - 2)$th (l.h.s. top) and proton $(N_f^{(p)} - 2)$th (l.h.s. bottom) single particle state respectively in ^{232}Th isotope as function of deformation parameter c and number of Gauss–Hermite integration nodes N_{GH} for NMAX $= 18$ shells. The same is plotted for neutron $(N_f^{(n)} + 2)$th and proton $(N_f^{(p)} + 2)$th states in the right panel. Meaning of $N_f^{(n)}$ and $N_f^{(p)}$ as in caption to Fig. 6.

one splits the total integration interval in each surface point, where $\vec{r}_1 = \vec{r}_2$ into two sub-intervals. This operation has in particular been applied for the domain in the vicinity of nuclear surface. On the other hand, for all contributions, where $|\vec{r}_1 - \vec{r}_2|$ is large, the factor $\exp(-|\vec{r}_1 - \vec{r}_2|/a)$ will be so small that their contribution to the total integral is practically negligible.

5. Input and output description

The input to the **yukawa.f** program is contained in the file **yukawa.inp**. Having compiled the code **yukawa.f** one can execute it using, e.g. the command **./yukawa < yukawa.inp > yukawa.out** in the Linux command line. Input parameters are read from that file using the NAMELIST/YPAR/ and NAMELIST/DANE/. Further on, they are transmitted to the main subroutine YUKA in COMMON blocks.

In the first namelist YPAR, the basic parameters of Table 1, determining the Yukawa-folded and spin–orbit potentials are

collected. On the basis of the latter, the rest of necessary parameters are calculated through Eqs. (54)–(56).

In the DANE namelist are collected those constants which can be freely changed, namely the nuclear charge ZNUC, the mass number ANUC of the considered nucleus and its deformations. The input parameter IFH selects between the Funny–Hills (IFH = 1) C,H,ALPHA and the Trentalange–Koonin–Sierk (IFH = 2) ALPH(1:NDTKS) shapes. The parameter NDTKS gives the number of TKS deformation parameters used in Eq. (9). Notice that the ETA deformation parameter describing nonaxial nuclear deformations is common for both the deformation-parameter sets. The input parameter IWF decides whether only energy eigenvalues (IWF = 0) of the Yukawa mean-field Hamiltonian, or eigenvalues and eigenvectors (IWF = 1) are generated.

The main parameters of the program, i.e. NMAX, NH, NDTKS as well as the numbers of the Gauss–Legendre integration nodes NG1, NG3 used to generate the Yukawa-folded and Coulomb potentials
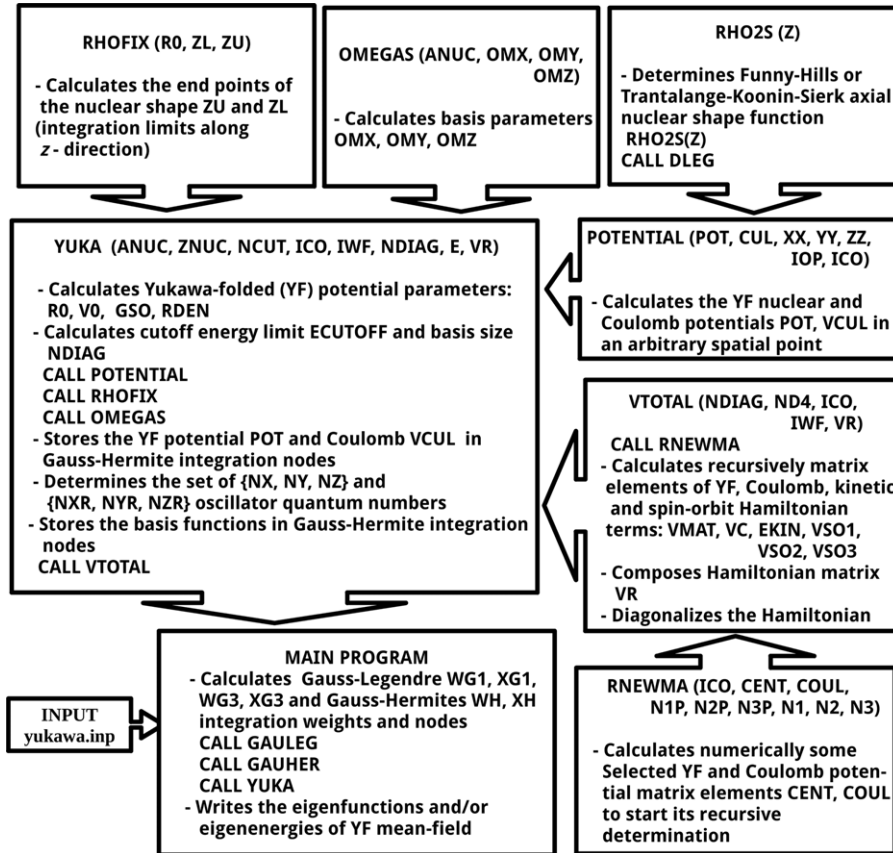
Fig. 8. Block diagram showing the organization of the *yukawa* program.

are put in PARAMETER statements in /**yuk-sizes** directory. They are called in individual subroutines by INCLUDE statement.

The parameter NCUT, corresponding to the quantity N_{cutoff} appearing in Eq. (87), denotes the **maximum** number of oscillator shells taken into account and determines the energy cut-off (87) beyond which no basis state is included in the diagonalization procedure. If the NCUT parameter is chosen sufficiently large, e.g. 100 or higher, then there is effectively no cut-off condition that allows to limit the number of oscillator basis states. A reasonable choice of NCUT is however already given by NCUT = 12.

The output appearing at the screen and copied to the file **levels.dat** contains, apart from the potential parameters of both namelists, the proton and neutron eigenenergies of the mean-field Hamiltonian printed in five columns. For a total number of NDX energy eigenvalues to be printed out, these are arranged, separately for protons and neutrons, in a field of 5 columns with NDX/5 eigenvalues each. In the attached output, NDX = 200 was chosen but its value can be adjusted freely by the user. If the parameter IWF is set to IWF = 1, also all NDIAG *normalized* orthogonal eigenvectors are printed out into the file **eigenfunctions.dat**. Such an eigenvector is uniquely determined by giving the expansion coefficients of that state in the basis states of Eq. (59). These expansion coefficients VR(i, k) give the contribution of basis state i to the eigenvector k according to the relation

$$\Psi_k(x, y, z) = \sum_{i=1}^{NDIAG} VR(i, k) \, | n_x(i), n_y(i), n_z(i), \Sigma(i) \rangle. \quad (91)$$

If for a certain reasons the explicit shape of the nth eigenstate $\Psi_n(x, y, z)$ is required, it can easily be constructed in this way.

Let us conclude by giving the reader an idea about the involved computation times:

For the eigensolutions of ^{208}Pb nucleus of spherical shape, with NMAX = 14 oscillator shells, the FH shape parametrization (IFH = 1) and the option (IWF = 1) of printing out the eigenvectors to the file **eigenfunctions.dat** requires about 7 s on an average dual-core 2 GHz notebook of 1 GB RAM memory.

The same kind of input, but for a rather complicated non-axial left–right asymmetric shape, as given e.g. by the FH parameters C = 1.4, H = 0.20, ALPHA = 0.3, and ETA = −0.15 requires approximately 11 s. Similar CPU times are obtained with the TKS shape parametrization.

6. Structure of the program

The program **yukawa.f** is coded in Fortran 77 with a double-precision representation of real numbers. Complex numbers do not appear in the entire program. This code of about 1770 lines long is composed of ten subroutines and two functions. The structure of the program is presented in Fig. 8.

7. Summary

The main purpose of the present work, and of the simple computer code that comes along with it, is the diagonalization of a single-particle Hamiltonian with a mean-field potential that is generated by a well known Yukawa-folding procedure, that has been applied successfully for over forty years now. The eigenvalue problem is solved in Cartesian coordinates by an expansion of the eigenvectors in the basis of a deformed harmonic oscillator. In its present form, the code is particularly destined to describe predefined elongated, necked-in, left–right asymmetric non-axial nuclear configurations, where the only imposed symmetry on the mean field is

the time reversal and the so-called z-signature symmetry. As already said, such kind of shapes occur in various nuclear processes, such as ground-state properties, giant resonances, as well as in any large-amplitude collective motions, like nuclear fission, fusion and heavy-ion reactions. The nuclear shapes are defined in cylindrical coordinates (but still allowing for non-axial deformations) by the Funny–Hills or the Legendre polynomial expression, referred here as Trentalange–Koonin–Sierk shapes. These shape parametrizations have proven to be flexible for the description of axial nuclear shapes along the path to fission, comparably with the widely used expansion in spherical harmonics (see e.g. [16] with maximum multipolarity $\lambda = 7$). As commonly known, the latter works well for nuclear shapes close to the ground state, but require too many deformation parameters for configurations close to the scission points.

Let us mention, however, that any shape parametrization could be easily incorporated into our code. In its present form, our code has the advantage that it practically does not impose any complicated symmetry restrictions, except time reversal and z-signature symmetry, as mentioned above.

The use of a nuclear Hamiltonian with a mean-field potential obtained by a Yukawa-folding procedure ensures not only that the volume of the nucleus is automatically conserved when the nucleus is deformed, a condition which would otherwise necessitate a *normalization* of the potential at each deformation which is always quite time-consuming in large-scale calculations. It also guarantees in addition a kind of selfconsistency between the nuclear density and the nuclear mean-field potential that generates the density, but which in turn, is determined by it, an effect that is not present in the competitive non-selfconsistent mean-field approaches.

Studying the structure of the code it becomes obvious that both the POTENTIAL and the RHO2Z subroutines, describing respectively the central potential as well as the nuclear surface shape, can easily be extended by adding other definitions of the central field and/or the nuclear shape, keeping the rest of the routines untouched. One has, however, to remember that any new surface parametrization that is incorporated into the program should always be able to generate shapes which show the required symmetries, i.e. time reversal and z-signature, otherwise more fundamental modifications of the code would be necessary. The other parts of the code, in particular the construction of the harmonic-oscillator basis states, the decomposition of the eigenstates of the Hamiltonian in the basis, the calculation of the resulting matrix elements and, finally, the diagonalization of the Hamiltonian, are completely general and could be used in connection with any nuclear shape and any analytically or numerically expressible mean-field potential.

Acknowledgements

References

[1] B. Nerlo-Pomorska, K. Pomorski, C. Schmitt, J. Bartel, Phys. Scr. 90 (2015) 114 010.
[2] J. Bartel, K. Pomorski, B. Nerlo-Pomorska, C. Schmitt, Phys. Scr. 90 (2015) 114 004.
[3] V.M. Strutinsky, Sov. J. Nucl. Phys. 3 (1966) 449; Nuclear Phys. A95 (1967) 420.
[4] M. Brack, J. Damgaard, A.S. Jensen, H.-C. Pauli, V.M. Strutinsky, C.Y. Wong, Rev. Modern Phys. 44 (1972) 320.
[5] S. Trentalange, S.E. Koonin, A.J. Sierk, Phys. Rev. C22 (1980) 1159.
[6] P. Möller, J.R. Nix, At. Data Nucl. Data Tables 59 (1995) 185–381.
[7] H.-C. Pauli, Phys. Rep. 7 (1973) 35.
[8] F. Ivanyuk, Phys. Scr. 89 (2014) 054012.
[9] V.M. Strutinsky, N.Y. Lyashchenko, N.A. Popov, Nuclear Phys. 46 (1963) 659.
[10] K. Pomorski, J. Bartel, Internat. J. Modern Phys. E15 (2006) 417.
[11] A. Bohr, Mat.-Fys. Medd. K. Dan. Vidensk. Selsk. 26 (14) (1952).
[12] K.T.R. Davies, J.R. Nix, Phys. Rev. C14 (1976) 1977.
[13] P.M. Morse, H. Feshbach, Methods of Theoretical Physics, Vol. 1, McGraw-Hill, New York, 1953, p. 464.
[14] V.A. Chepurnov, Yad. Fiz. 6 (1968) 955; Nuclear Phys. A435 (1985) 397.
[15] U. Götz, H.-C. Pauli, K. Alder, Nuclear Phys. A175 (1971) 481.
[16] M. Kowal, P. Jachimowicz, A. Sobiczewski, Phys. Rev. C82 (2010) 014303.